# Epithelial-derived TGF-β2 modulates basal and wound-healing subepithelial matrix homeostasis

**H. Garrett R. Thompson,[1] Justin D. Mih,[1] Tatiana B. Krasieva,[3]
Bruce J. Tromberg,[1,3,4] and Steven C. George[1,2]**

[1]*Department of Biomedical Engineering,* [2]*Department of Chemical Engineering and Materials Science,*
[3]*Beckman Laser Institute, and* [4]*Department of Surgery, University of California, Irvine, Irvine, California*

**Thompson, H. Garrett R., Justin D. Mih, Tatiana B. Krasieva, Bruce J. Tromberg, and Steven C. George.** Epithelial-derived TGF-β2 modulates basal and wound-healing subepithelial matrix homeostasis. *Am J Physiol Lung Cell Mol Physiol* 291: L1277–L1285, 2006. First published August 4, 2006; doi:10.1152/ajplung.00057.2006.—The epithelium influences the mesenchyme during dynamic processes such as embryogenesis, wound healing, fibrosis, and carcinogenesis. Since transforming growth factor-β (TGF-β) modulates these processes, we hypothesized that epithelial-derived TGF-β also plays a critical role in maintaining the extracellular matrix at basal conditions. We utilized an in vitro model of the epithelial-mesenchymal trophic unit in the human airways to determine the role of epithelial-derived TGF-β in modulating the extracellular matrix under basal and wound-healing conditions. When differentiated at an air-liquid interface, the human bronchial epithelium produces active TGF-β2 at a concentration of 50–70 pg/ml, whereas TGF-β1 is undetectable. TGF-β2 increases two- to threefold following scrape injury in a dose-dependent fashion and significantly enhances both α-smooth muscle actin expression in the underlying collagen-embedded fibroblasts and secretion of tenascin-C into the matrix. Multiphoton microscopy demonstrates substantially enhanced second harmonic generation from fibrillar collagen in the matrix. Pretreatment of the matrix with either sirolimus (2.5 nM) or paclitaxel (10 nM) abolishes the increases in both TGF-β2 and second harmonic generation in response to epithelial injury. In the absence of the epithelium, exogenous active TGF-β2 (0–400 pg/ml) produces a biphasic response in the second harmonic signal with a minimum occurring at the epithelial-derived basal level. We conclude that epithelial-derived TGF-β2 is secreted in response to injury, significantly alters the bulk optical properties of the extracellular matrix, and its tight regulation may be required for normal collagen homeostasis.

extracellular matrix; airway; fibrosis; multiphoton microscopy; fibroblast

---

THE EPITHELIUM IS KNOWN TO drive mesenchymal tissue development during embryogenesis (40) in numerous organ systems, and these processes may be activated in the adult in both normal and disease states. Injury and disease can compromise the epithelial barrier and lead to the secretion of soluble factors, which can modulate the underlying mesenchyme and influence tissue growth and remodeling. This can be part of a normal wound-healing response or can involve pathological processes leading to excess tissue growth such as fibrotic scarring and carcinogenesis. The role of the epithelium in maintaining basal mesenchymal tissue architecture, when wound-healing processes have not been activated, has received less attention. However, if epithelial-derived mediators can influence the mesenchyme during normal wound healing or disease, it is reasonable to hypothesize that these same processes may also modulate the extracellular matrix under basal conditions.

In reference to the lungs, the airway epithelium and underlying mesenchyme have been dubbed the epithelial-mesenchymal trophic unit (EMTU) (21), which has been gaining steady attention as a key regulator of structural changes observed in diseases such as asthma, interstitial lung fibrosis, and cancer (14, 15, 22, 24, 25, 27–29, 32, 50). However, this concept is not limited to the lung, and the dynamic and reciprocal relationship between the epithelium and the mesenchyme is relevant to a broad range of organ systems including the eye (56), skin (4), digestive (34, 37, 52), breast (11), prostate (5), and cardiovascular systems (10). Transforming growth factor-β (TGF-β) and its receptors are prominent mediators of cell function and tissue growth, including the EMTU. Although TGF-β has three isoforms, TGF-β2 appears to be the prominent isoform expressed in the airways (3, 41, 51). Epithelial-derived TGF-β2 in the airway is increased following epithelial insult (41, 51) and can modulate subepithelial fibroblast function (35, 51). Thus it is thought to be a prominent mediator of EMTU function in the airways. However, it is not known, under basal or wound-healing conditions, whether epithelial-derived TGF-β2 actually modulates changes in the extracellular matrix.

We hypothesized that the airway epithelium influences the underlying fibroblast under both basal and injury conditions leading to changes in the structure and composition of the extracellular matrix. Although a TGF-β2 null mouse would be an intriguing model to investigate the basal role in the airway EMTU, these animals exhibit perinatal mortality due to multisystem defects (46). Thus to test our hypothesis, we utilized an in vitro model of the airway EMTU using commercially available primary human airway epithelial cells and lung fibroblasts embedded within a collagen matrix. Using a combination of techniques to probe not only protein expression in the epithelial and fibroblast cells, but also the structure of the extracellular matrix itself using multiphoton microscopy, we demonstrate that epithelial-derived TGF-β2 modulates the basal structure of the extracellular matrix, as well as the epithelial injury response, over a relatively small range of concentration (50–150 pg/ml). Together, these data suggest that tight regulation of TGF-β2 is required for extracellular matrix homeostasis.

---

Address for reprint requests and other correspondence: Steven C. George, Dept. of Biomedical Engineering, 3120 Natural Sciences II, Univ. of California, Irvine, Irvine, California 92697–2715 (e-mail: scgeorge@uci.edu).

## METHODS

*Chemicals and reagents.* Recombinant human TGF-β1, TGF-β2, and anti-TGF-β2 neutralizing antibody were purchased from R&D Systems (Minneapolis, MN). Human VEGF, TGF-β1, and TGF-β2 were measured from the conditioned media by ELISA in 96-well plate format per the manufacturer's instructions (R&D Systems). Sirolimus and paclitaxel were gifts from Broncus Technologies (Mountain View, CA). All other chemicals were from Sigma (St. Louis, MO) unless specified otherwise.

*Cell culture and tissue model.* Primary normal human lung epithelial cells (NHBE) and primary normal human lung fibroblasts (NHLF) were purchased from Cambrex (Walkersville, MD) and cultured in the recommended media, bronchial epithelial growth medium (BEGM) and Fibroblast Growth Media-2 (FGM-2) (Cambrex), respectively, prior to coculture. Twelve-well tissue culture dishes and uncoated 0.4-μm pore Transwell inserts were purchased from Corning Costar (Costar, Cambridge, MA). NHBEs were expanded twice and thus used at *passage 3*. The NHBE were then seeded at a density of 150,000 cells/cm$^2$ directly on top of a Transwell polyester membrane. The cells were submerged in media for 5 days to allow attachment and confluence. For the first 48 h, the media was BEGM with low retinoic acid concentration, after which media was replaced with 50:25:25 mixture of BEGM:DMEM:Ham's-F-12 with a high retinoic acid concentration and an additional BEGM bullet kit. At *day 6*, an air-liquid interface was established and the epithelium was allowed to differentiate for 2 wk.

Stocks of NHLF were used between *passages 5* and *7*. Cells were routinely cultured as a monolayer in 75-cm$^2$ flasks (Falcon Labware, Oxnard, CA) or 10-cm culture dishes (Costar) in the recommended media until 60–70% confluent and then passaged at 1:5 dilution. The NHLF were seeded in 1.7 mg/ml of rat tail tendon collagen I (Collaborative, Bedford, MA), DMEM, and reconstitution buffer (25 mM NaHCO$_3$, 20 mM HEPES, and 5.0 mM NaOH). Aliquots of the mixture containing 50,000 cells per tissue were pipetted onto sterile 250-μm polypropylene meshes (Small Parts, Miami Lakes, FL) for structural support. The collagen mixture was then noncovalently cross-linked at 37°C in 5% CO$_2$ for 0.5–3 h, creating the NHLF tissue. One milliliter of FGM-2 was then added to each well for 24 h and then replaced with 50:25:25 media. In some experiments, the Transwells containing the fully mucociliary differentiated NHBEs were added to the freshly made collagen-embedded fibroblast matrices creating the NHBE-NHLF tissue.

Epithelial injury was induced by mechanically denuding the full diameter of a Transwell with a 100-μl pipette tip (diameter of tip ~500 μm). Unless otherwise noted, an injury refers to a single scrape, repeated four times at 48-h intervals, to an NHBE-NHLF tissue. In some experiments only a single one-time scrape was employed, while in others three simultaneous scrapes were used. For the latter, subsequent insults were made at 45° angles. For TGF-β and VEGF ELISAs, conditioned media was collected at 48-h intervals just prior to scrape and replaced with media as indicated. Uninjured tissues were treated identically. Samples used for transepithelial electrical resistance (TER) measurements were not used for subsequent experiments, as apically secreted molecules were necessarily diluted and removed by the addition of media to the top compartment prior to measurements using an ohmmeter (Millicell-ERS; Millipore, Bedford, MA).

*SDS-PAGE and Western blots.* Collagen-embedded fibroblast matrices were lysed on ice in radioimmunoprecipitation assay (RIPA) buffer (50 mM Tris, pH 8.0, 150 mM NaCl, 1.0% Nonidet P-40, 0.5% sodium deoxycholate, 0.1% SDS, 0.1 mM sodium orthovanadate) supplemented with protease inhibitor cocktail (Sigma) by repetitive scraping. Protein concentrations were determined by addition of Bradford dye modified for use with detergents (Bio-Rad, Hercules, CA) (8). Laemmli sample buffer (5 μl) was added to 15 or 40 μg protein diluted in gel running buffer prior to boiling for 5 min. Samples were subjected to SDS-PAGE and transferred to nitrocellu-lose. Western blot analysis was performed using standard methodology including appropriate primary and horseradish peroxidase (HRP)-conjugated secondary antibodies. Monoclonal mouse anti-tenascin-C (anti-TnC) and anti-α-smooth muscle actin (anti-α-SMA) were from Sigma and diluted 1:1,000 and 1:400, respectively. Mouse monoclonal anti-β-actin and HRP-conjugated sheep anti-mouse IgG secondary antibody (Abcam, Cambridge, UK) were both diluted 1:2,000.

*Immunofluorescence microscopy.* At the point of coculture experimentation, some wells of mucociliary differentiated NHBE were fixed and permeabilized with Triton X-100. Nonspecific binding was blocked by the addition of 10% goat serum and 1% BSA in PBS, and samples were subsequently rinsed with PBS. Samples were incubated in mouse anti-mucin (MUC5AC) or anti-β-tubulin IV (Sigma) at 1:1,500 dilution, rinsed with PBS, and incubated in Alexa Fluor 488 anti-mouse secondary antibody (Molecular Probes, Eugene, OR) at 1:1,000 in PBS. Cell nuclei were counterstained with 4,6-diamidino-2-phenylindole (DAPI; Molecular Probes) at 300 nM for 4 min. After staining, cells were rinsed four times with PBS, the Transwell membranes were removed by scalpel, placed on a microscope slide with a drop of Vectashield, and visualized using a Nikon Eclipse E800 epifluorescence microscope.

*Multiphoton microscopy.* The density of collagen fibers was studied in the extracellular matrix of the fibroblast tissue model using multiphoton microscopy (MPM) as previously described (1, 57). Briefly, collagen-embedded NHLF matrices were lifted onto microscope slides and covered with full-length coverslips, thinness 1 (Fisher Scientific, Pittsburgh, PA), and excited with a 100-fs Titanium:Sapphire laser as the multiphoton excitation source. An excitation wavelength of 780 nm was used to generate emitted second harmonic light at 390 nm and visualized using a Zeiss Meta 510 inverted microscope. Second harmonic generation (SHG) is specific to the noncentrosymmetric structure of fibrillar collagen (61).

Tissues were imaged over a 35 μm × 35 μm scan region, integrated over 8–16 scans, at multiple depths within the tissue (5- to 20-μm intervals, using a ×40 oil-immersion objective with a working distance of 250 nm). Resolution was ~0.4 μm in *x*-, *y*-, and 1 μm in *z*-image planes, with an area of 0.019 μm$^2$ per pixel. The mean SHG signal intensity at each depth of the tissue, S(z), was then calculated using pixels demonstrating a positive SHG signal (i.e., background signal intensity pixels were removed to control for void spaces). The SHG signal decays exponentially with depth (1) due to scattering of both excitation and emitted backscattered light such that $S(z)/S(0) = \exp(-z/L_{scat})$ where $L_{scat}$ is the decay length constant and S(0) is the maximum signal intensity (denoted z = 0). Data is presented using both S(0) as well as $L_{scat}$ determined as the negative inverse of the slope from a linear regression of $\ln[S(z)/S(0)]$ vs. z.

## RESULTS

Primary epithelial cells cultured on Transwells underwent mucociliary differentiation during the 14 days at an air-liquid interface. Representative immunofluorescence images of epithelial cultures imaged en face using anti-mucin (MUC5AC), anti-β-tubulin IV, and anti-ZO-1 antibodies illustrate the presence of mucus-producing cells (goblet cells), ciliated cells, and tight junction formation, respectively (Fig. 1).

Repetitive epithelial denudation by scrape injury induced unrecoverable changes in the electrophysiological properties of the epithelium, altered protein expression in the subepithelial fibroblasts, and modulated the bulk optical properties of the extracellular matrix. Figure 2*A* shows the effect of wounding on the TER from one representative experiment of 12 unwounded and 12 wounded NHBE tissues. Repetitive epithelial denudation significantly reduces the TER relative to control, and, in NHBE-NHLF tissues, increases the protein content of α-SMA and TnC by approximately twofold in the collagen-
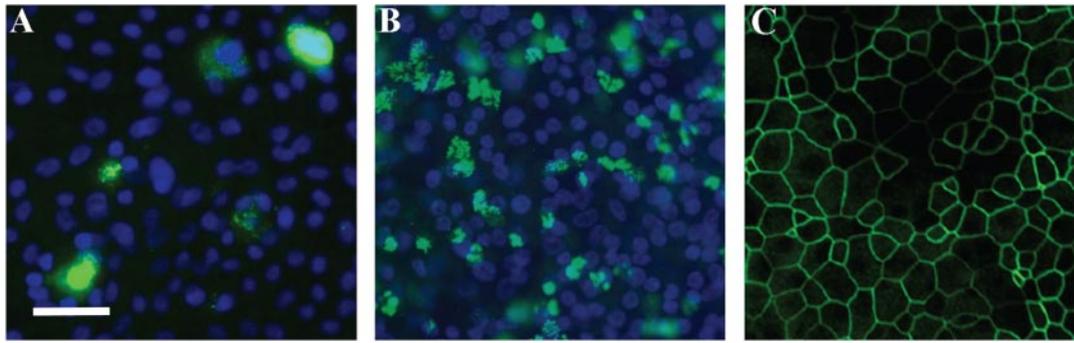
Fig. 1. Mucociliary differentiation of epithelial monolayers. Immunofluorescence illustrating the presence of mucus with anti-MUC5AC (*A*), cilia with anti-β-tubulin IV (*B*), and tight junctions with anti-zonula occludens-1 (*C*). Nuclei were stained with 4,6-diamidino-2-phenylindole (DAPI). Images were taken using a ×40 objective (scale bar is 50 μm).

embedded fibroblasts and matrix, respectively (Fig. 2, *B* and *C*). Figure 2*D* illustrates that repetitive epithelial injury enhances the SHG signal, an index of collagen fibril organization and density, from collagen in the underlying extracellular matrix near the surface, and increases the rate of decay of the SHG signal with depth ($L_{scat}$ decreases from 28.3 to 16.3 μm). Both of these observations are consistent with increased collagen fibrillar organization and density in the matrix. The
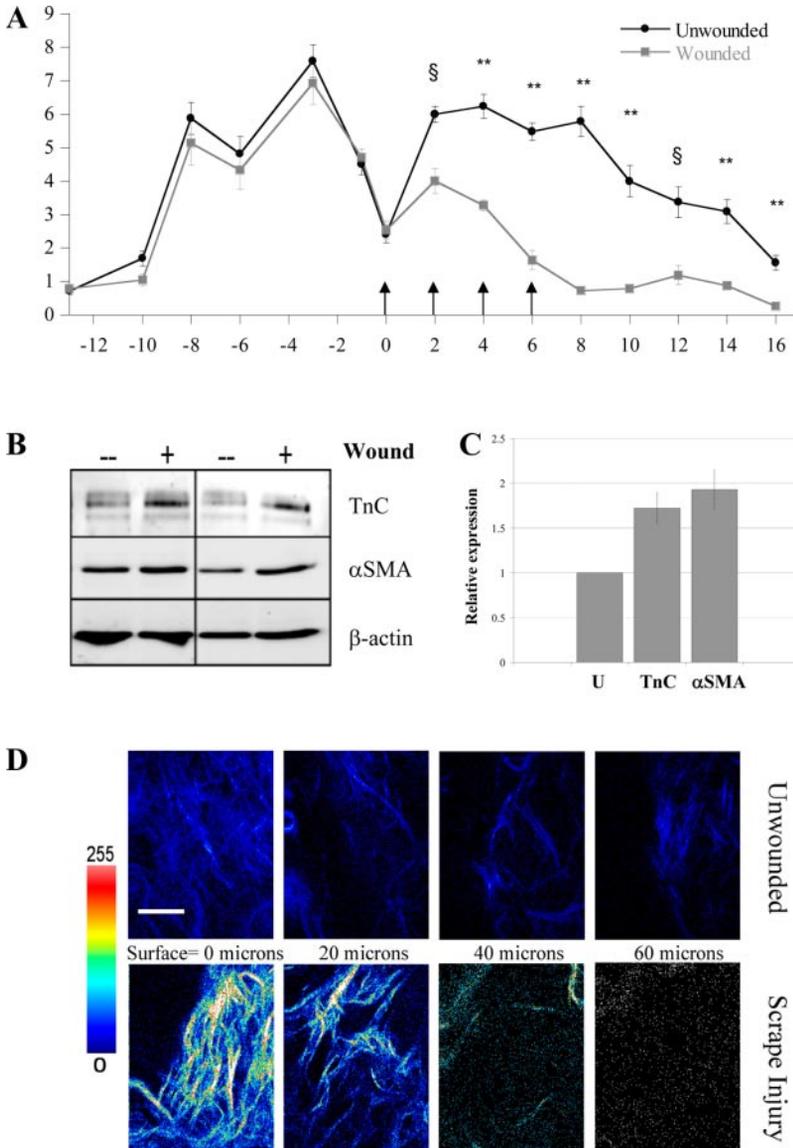


Fig. 2. Epithelial denudation alters electrophysiological properties of the epithelium and matrix composition, and signals myofibroblast differentiation. *A*: transepithelial electrical resistance (TER) values of 12 unwounded (●) and 12 wounded (■) epithelial layers from the first day of air-liquid interface (*day 7* in culture). Arrows indicate days of wounding on *days 0, 2, 4*, and *6*. Data presented are means ± SE. §$P < 0.001$; **$P < 10^{-6}$. *B*: an amount of 15 μg total protein analyzed by Western blot for α-smooth muscle actin (SMA), TnC (tenascin-C, short isoform 180–220 kDa), and β-actin control from 2 separate experiments in the absence or presence of repetitive mechanical epithelial injury. *C*: densitometric quantitation from 3 independent experiments assayed in duplicate. Data presented are means ± SD. *D*: representative second harmonic generation (SHG) of the ECM from unwounded (top panels) and wounded tissue (bottom panels) 10 days after the final injury, as a function of depth into the tissue construct. Scale bar is 10 μm. U, unwounded.

representative data in Fig. 2D illustrates that at a tissue depth of 60 μm, no SHG signal can be detected from collagen I in wounded tissue, whereas the signal from the unwounded tissue is still visible.

To investigate the underlying mechanism of the changes in the subepithelial fibroblasts and matrix following epithelial injury, we analyzed the conditioned media for active TGF-β1 and TGF-β2 from wounded epithelial monolayers and unwounded and wounded NHBE-NHLF tissues. While TGF-β1 was not detectable ($<7$ pg/ml) in this model system (data not shown), the basal concentration of active TGF-β2 from the NHBE alone was ~50–70 pg/ml over the experimental time course (Fig. 3, first panel). Epithelial denudation, either in the absence (Fig. 3, panels 2 and 3) or presence (Fig. 3, panel 4) of NHLF, significantly increased epithelial-derived active TGF-β2 in a dose-dependent manner (e.g., magnitude of scrape in terms of number of scrapes). Elevated levels of active TGF-β2 were sustained following the last scrape injury only in the presence of the collagen-embedded fibroblasts (Fig. 3, panel 4).

To examine whether the increased concentration of active TGF-β2 could account for the effects on the fibroblasts and matrix observed with epithelial wounding (Fig. 2), NHLF tissues (in the absence of an epithelium) were subjected to a range of exogenous TGF-β2 doses from 0–400 pg/ml for 14 days with fresh media and growth factor added at 48-h intervals. While little, if any, change in α-SMA was evident, TnC protein expression was significantly elevated when subjected to at least 150 pg/ml active TGF-β2 (Fig. 4, A and B). The threshold of ~150 pg/ml is achieved with multiple epithelial scrape injuries (Fig. 3), suggesting that the wound-induced increase in soluble active TGF-β2 is responsible for the in-creased TnC, but not α-SMA, seen under those conditions. Figure 4C demonstrates a biphasic response of the SHG signal with TGF-β2. The basal concentrations of active TGF-β2 from the NHBE (50–70 pg/ml) produces a minimum in the SHG signal at the surface of the matrix (and a maximum in $L_{scat}$, data not shown). Interestingly, the absence of exogenous TGF-β2 in NHLF tissues induces an SHG signal that is comparable with 200 pg/ml and is approximately fourfold higher than the minimum.

The observation of the biphasic response in the SHG signal prompted us to investigate the role of basal TGF-β2 from the epithelium in subepithelial matrix homeostasis. Neutralizing active TGF-β2 in unwounded NHBE-NHLF tissues increased TnC expression to wounded tissue levels but did not alter expression in wounded tissues (Fig. 5A). In contrast, the neutralizing antibody had no impact on α-SMA expression in unwounded NHBE-NHLF tissues, but had a modest effect on α-SMA expression in wounded tissues (Fig. 5A). Mirroring the effect seen in NHLF tissues, exogenous active TGF-β2 en-hances the SHG signal at the surface in unwounded NHBE-NHLF tissues (Fig. 5, B and C). However, addition of the neutralizing antibody markedly enhanced the SHG signal (Fig. 5B) consistent with the zero dose of TGF-β2 in Fig. 4C.

To further investigate the role of epithelial-derived TGF-β2 on matrix homeostasis, we exposed NHBE-NHLF wounded and unwounded tissues to the antiproliferative drugs sirolimus and paclitaxel. Tissues pretreated with either drug had a sig-nificantly decreased concentration of active TGF-β2 in the conditioned media (Fig. 6A). However, the bioavailability of active TGF-β2 was not abolished. When drug-treated tissues were wounded, no increase in active TGF-β2 was observed; levels remained identical to drug-treated unwounded values, on
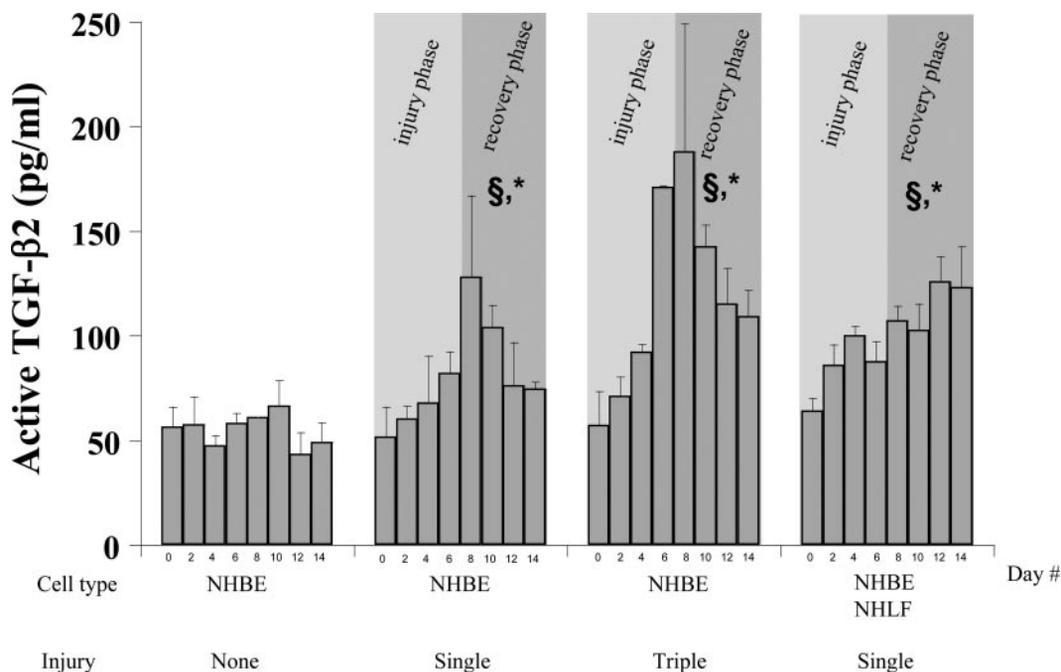


Fig. 3. Epithelial denudation increases active TGF-β2. Active transforming growth factor-β2 (TGF-β2) levels (pg/ml) from 2 experiments with 3–6 tissues per time point per experiment. Basal TGF-β2 concentration is static over the time course in the coculture tissue model (first panel). A single scrape (panel 2) or triple scrape (panel 3) was applied to the epithelium in the absence of collagen-embedded fibroblasts at 48-h intervals. Single scrape denudation of the epithelium in the coculture model (panel 4) illustrates sustained elevation of active TGF-β2 levels. Maximum effect compared with baseline §$P < 0.001$; mean of recovery phase different from mean of injury phase, *$P < 0.02$. NHBE, normal human lung epithelial cells; NHLF, normal human lung fibroblasts.
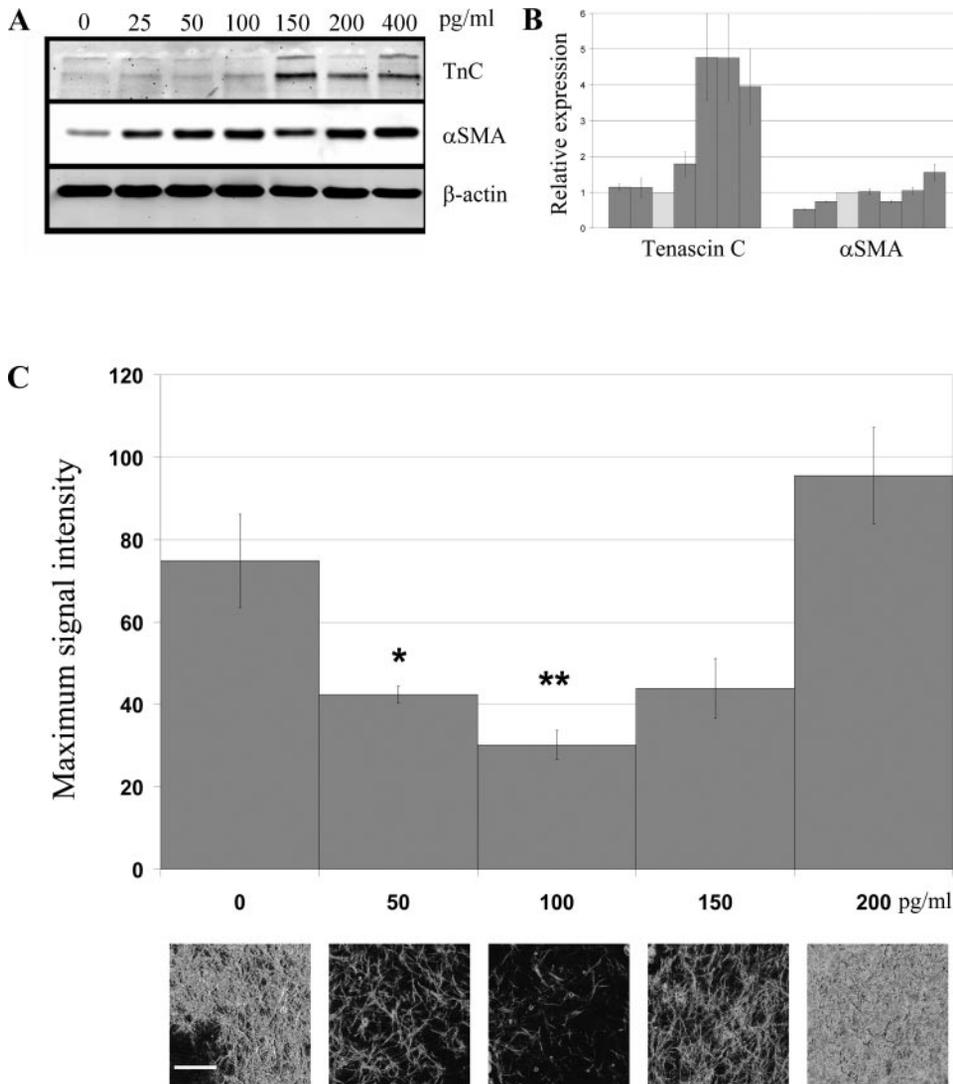
Fig. 4. Exogenous TGF-β2 at physiological doses induces TnC expression and collagen matrix reorganization. *A*: representative Western blot analyses of 15 μg total protein for α-SMA and TnC, short isoform 180–220 kDa) from two experiments treating collagen-embedded NHLF cultures with the indicated dose of active TGF-β2. β-Actin is presented to show equal loading. *B*: expression levels normalized to 50 pg/ml dose (light gray), indicating approximate basal concentration seen in coculture model. *C*: representative SHG images of surface collagen fibrils for each dose of exogenous active TGF-β2 are presented below the quantitation of signal intensities. Three to five fields of view for 3 tissues were imaged at each concentration to generate mean values ± SE. *$P < 0.02$; **$P < 0.005$, relative to "0 dose." Scale bar is 10 μm.

average, over the experimental time course. Unlike wounded tissues, in which the increase in epithelium-derived active TGF-β2 is concomitant with enhanced surface SHG signal, drug-treated wounded tissues exhibited a collagen matrix indistinguishable from unwounded controls (Fig. 6, *B* and *C*). Further investigation determined that the decreases in active TGF-β2 seen with either sirolimus or paclitaxel treatment were responsible for the change in collagen fibril formation, as addition of exogenous active TGF-β2 recovered the enhanced surface SHG signal (Fig. 6, *B* and *C*).

## DISCUSSION

Bronchial asthma afflicts 5–10% of the population, and, despite significant resources to understand the pathogenesis, the prevalence of this disease remains high (17, 42). A prominent feature of the disease is subepithelial fibrosis, which is characterized by the deposition of extracellular matrix proteins, including fibrillar collagens, fibronectin (FN), and TnC, among others. This increase in matrix protein synthesis has long been attributed to an increase in myofibroblasts (23), whose presence has been described in practically all fibrotic situations characterized by tissue retraction and remodeling (see Ref. 16

for review). The current study has investigated the role of epithelial-derived TGF-β2 in modulating subepithelial fibrosis using an in vitro model of the airway EMTU. By combining traditional methods to assess protein expression with multiphoton imaging, our results demonstrate that TGF-β2 impacts the regulation of TnC expression and collagen organization in the matrix under basal condition, and that epithelial injury can increase the concentration of TGF-β2 by approximately twofold and induce changes in the matrix that are consistent with subepithelial fibrosis. The results suggest a prominent role for the epithelium in modulating basal matrix homeostasis and that tight regulation of epithelial-derived TGF-β2 may be necessary for normal EMTU function.

Advances in primary cell culture techniques provide new opportunities to develop in vitro tissue models of cell-cell communication and angiogenesis relevant to asthma. Our three-dimensional (3-D) system is similar to models that have been previously presented to examine EMTU communication (13, 48, 51) and was designed specifically to examine soluble mediators generated in response to epithelial desquamation on matrix-embedded fibroblast activity and modulation of the extracellular matrix. Although many facets of in vivo biology
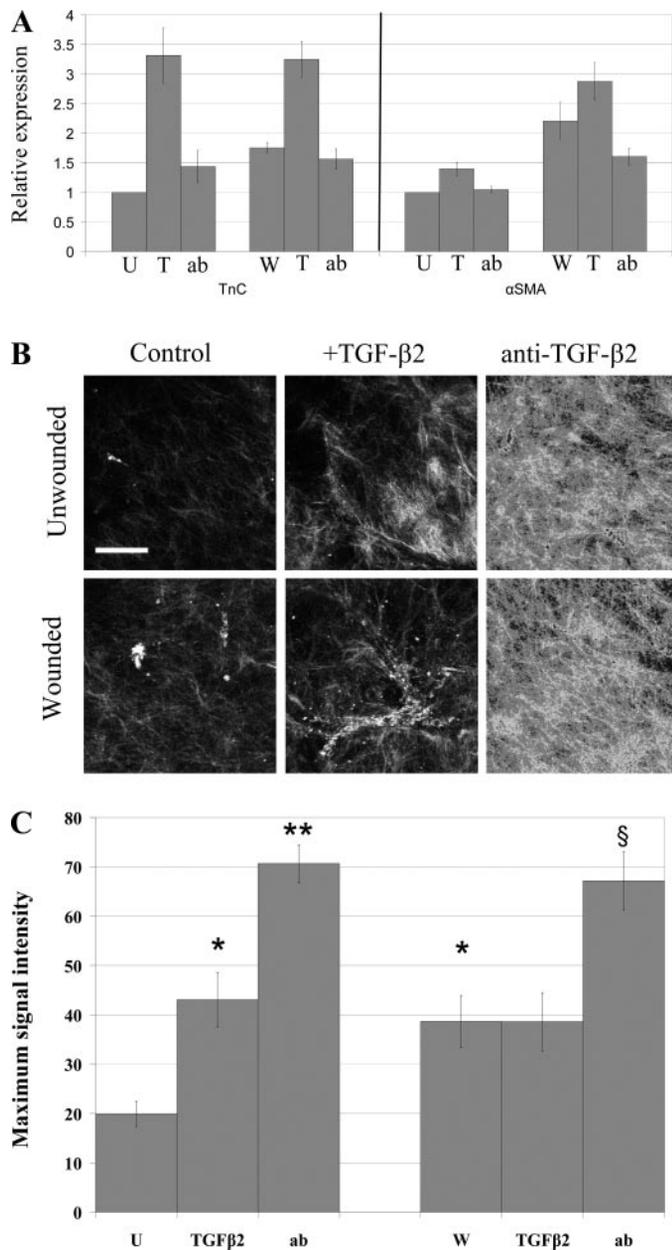
in this study mimics key features of the respiratory mucosa, including a differentiated epithelium with epithelial barrier integrity, mucus secretion, and cilia (Fig. 1); matrix-embedded pluripotent lung fibroblasts that differentiate and secrete struc-
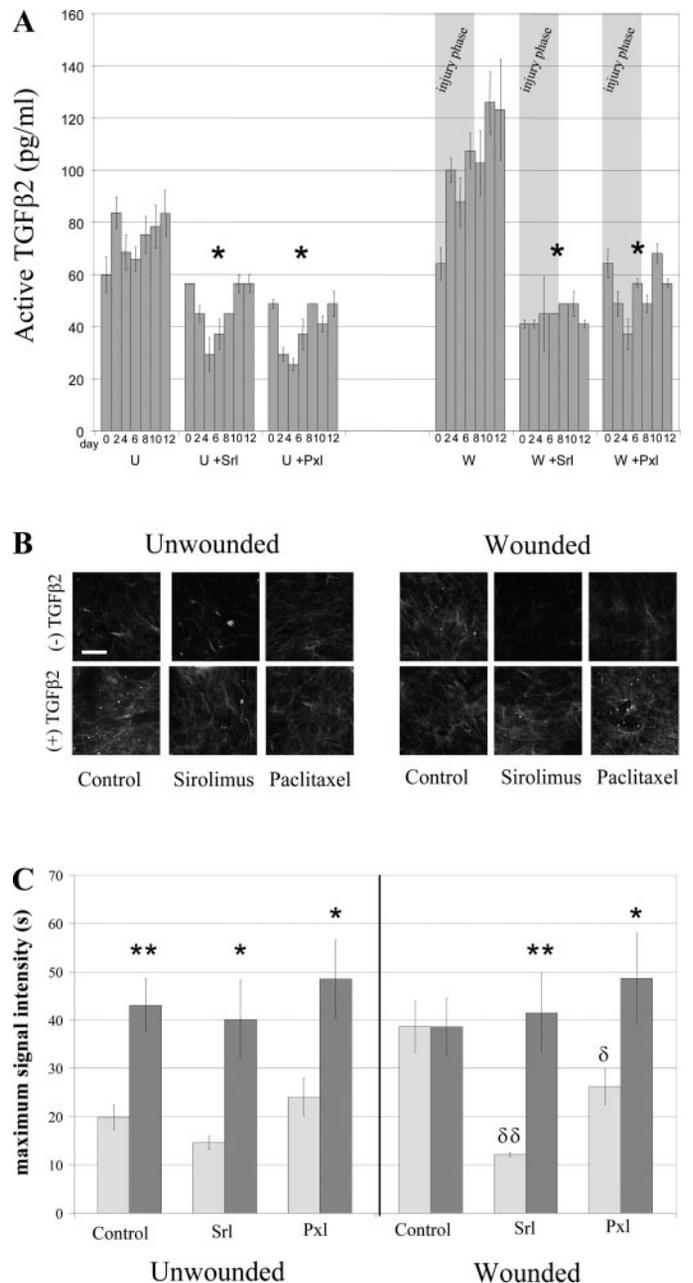


Fig. 5. TGF-β2 neutralizing antibody enhances collagen matrix reorganization but not TnC protein expression. An amount of 400 pg/ml active TGF-β2 (T) or 2 μg/ml anti-TGF-β2 neutralizing antibody (ab) were added to unwounded (U) or wounded (W) NHBE/collagen-embedded NHLF coculture tissues. *A*: quantitation of wound- and TGF-β2-induced increases in TnC protein expression by Western blot from 2 separate experiments, assayed in duplicate. *B*: representative SHG images of surface collagen fibrils from unwounded and wounded tissue in the presence or absence of exogenous active TGF-β2 or neutralizing antibody. *C*: quantitation of maximum signal intensity. Three to five fields of view for 3 tissues were imaged at each concentration to generate mean values ± SE. Relative to unwounded control, *$P < 0.005$; **$P < 10^{-9}$. Relative to wounded control, §$P < 0.005$. Scale bar is 10 μm.

Fig. 6. Sirolimus (Srl) and paclitaxel (Pxl) inhibit fibrosis by inhibiting wound-induced active TGF-β2 levels. Coculture tissues were pretreated with either 2.5 nM Srl or 10 nM Pxl prior to mechanical scrape injury. *A*: active TGF-β2 levels were measured in the conditioned media from unwounded (U) or wounded (W) tissues from 2 experiments with 3–6 tissues per time point per experiment. Mean values of drug treated tissues across the experimental time course are significantly different (*$P < 2 \times 10^{-4}$), relative to appropriate U or W controls. *B*: representative SHG images of surface collagen fibrils from unwounded and wounded tissues in the absence or presence of exogenous TGF-β2, Srl, or Pxl. *C*: quantitation of SHG signal intensities from 3–5 fields of view for 3 tissues of each condition. Mean values ± SE. Relative to (−)TGF-β2 control, *$P < 0.05$, **$P < 0.001$. Relative to wounded control, δ$P < 0.05$, δδ$P < 0.001$. Scale bar is 10 μm. Dark gray bars represent +400 pg/ml TGF-β, and light gray bars represent control.

cannot be replicated in self-polymerizing gels, including ECM molecular composition, protein diversity, and the heterogeneous structure of the tissue, 3-D model systems have clear advantages over 2-D culture systems. In particular, they more closely mimic in vivo conditions, allowing study of specific factors under more physiological conditions with respect to dimensionality, architecture, and cell polarity. The model used

tural extracellular matrix proteins (Figs. 2, 4, and 5); and a 3-D spatial orientation of the fibroblast ECM layer. Additionally, epithelial injury induces fibrillar collagen organization, myofibroblast differentiation, and TnC protein (Figs. 2 and 5), all similar to the fibrotic response seen in vivo.

In addition to reporting changes in protein expression profiles, we quantified subepithelial fibrosis in terms of a structural reorganization of the ECM, in this case collagen I. MPM utilizes pulses of NIR, which are minimally scattered in living tissue (1); thus MPM is an effective technique for imaging relatively thick tissues (100–500 μm). The noncentrosymmetric structural features of collagen produces nonlinear interactions between the focused laser beam and collagen fibrils leading to SHG at exactly half of the excitation wavelength (26, 61). This is a bulk effect of the surface layers of polymerized collagen (55), and thus the intensity of the SHG light at the source is a positive function of both the amount of the collagen and the relative organization. Because the light captured by the photomultiplier tube represents backscattered light, the SHG signal decreases with depth into the tissue (18, 61). Thus in the current study, the biphasic response of the SHG signal at the surface of the tissue suggests that basal concentrations of TGF-β2 act to minimize the structural organization or concentration of collagen.

Epithelial repair after desquamation can modulate fibroblasts leading to alterations in the underlying airway mesenchyme. For example, epithelial-derived chemotactic and mitogenic stimuli stimulate fibroblast migration, proliferation, transition to a myofibroblast phenotype, and production of the extracellular matrix (2, 9, 36, 43, 47). In fact, several studies demonstrated elevated tissue collagen content correlating with increased collagen fiber formation in conjunction with a greater number of interstitial myofibroblasts (16, 19, 23). Of importance in this process are the TGF-β family members. It has been demonstrated that human bronchial epithelial cells can produce TGF-β2 at levels that alter gene expression and migration of fibroblasts (35, 41, 51). In addition, the immune response has been implicated in tissue remodeling. Whether TGF-β2 is derived from eosinophils at sites of fibrosis (3) or cytokines regulate bronchial epithelium-derived TGF-β2 (44, 53, 54), TGF-β2 release contributes to both normal airway repair and to the development of subepithelial fibrosis in asthma. To the best of our knowledge, this is the first report demonstrating that basal concentrations of TGF-β2 modulate subepithelial collagen matrix homeostasis.

TnC is a developmentally regulated matrix protein that modulates cellular responses to other matrix proteins, such as FN. TnC is secreted by myofibroblasts, and its presence in the matrix may also recruit and further stimulate the differentiation of the myofibroblast (49). TnC colocalizes with α-SMA immunoreactivity and sites of fibrosis in not only asthmatic subepithelial fibrosis (45) but also neonatal respiratory distress syndrome, bronchopulmonary dysplasia, and usual interstitial pneumonia (30, 31, 38). TnC is not expressed to any significant degree in the normal lung under basal conditions; however, our in vitro model expresses TnC at basal conditions (Figs. 2B and 4A), which is consistent with the presence of myofibroblasts. Although the neutralizing TGF-β2 antibody impacted basal TnC levels, it did not significantly alter expression following wounding (in sharp contrast to the SHG signal and collagen organization). This observation suggests that collagen organi-

zation is more dependent on TGF-β2 levels than TnC expression following epithelial injury. TnC exists in alternatively spliced isoforms, with the long form containing fibronectin type III repeats present during wound repair, tumor formation, and embryonic development (12, 20, 33, 58). In the present study, the short isoform was detectable by RT-PCR, whereas the long isoform could not be detected with either wounding or exogenous addition of active TGF-β2 (data not shown). These results are consistent with the Western blot data demonstrating the presence of the short splice variants (180–220 kDa) but not the large 320-kDa isoform.

Sirolimus (rapamycin) and paclitaxel (taxol) are both small, lipophilic, chemically stable cell cycle inhibitors with antiproliferative properties (39). Paclitaxel is used as a chemotherapeutic to prevent tumor growth. The antiproliferative effect of paclitaxel is attributed to the stabilization of microtubules, which can antagonize TGF-β. For example, in acute lung injury, TGF-β induces actin cytoskeleton remodeling, resulting in endothelial cell barrier dysfunction. This is due to partial dissolution of peripheral microtubules and decreased levels of stable acetylated microtubules, an effect that is attenuated by stabilizing microtubules with paclitaxel (7). Another study shows that paclitaxel reverses the TGF-β mediated inhibition of myogenesis, as this process occurs via Smad-microtubule interaction (60). Like these studies, our results demonstrate clear antagonism between paclitaxel and TGF-β2.

Sirolimus is used as an immunosuppressant to prevent transplant rejection. It blocks the cell cycle in the late G1 stage by inhibiting the phosphorylation of mammalian target of rapamycin (mTOR). Prevention of liver fibrosis by sirolimus was first demonstrated in rats exposed to long-term treatment with CCl4 (59). Using a bile duct-ligated rat as a model of liver fibrosis, it was found that 28-day treatment of sirolimus reduced TGF-β mRNA and protein levels and inhibited fibrosis (6). Whereas it is unknown whether TGF-β2 mRNA or total protein levels are affected by sirolimus in the current model, it is clear that the amount of bioavailable active TGF-β2 is reduced and treatment of the tissue with sirolimus inhibits the wound-induced increase in TGF-β2.

In conclusion, this study has investigated the role of epithelial-derived TGF-β2 in modulating subepithelial extracellular matrix homeostasis using an in vitro model of the airway EMTU. By combining traditional methods to assess protein expression with multiphoton imaging, our results demonstrate that TGF-β2 regulates TnC protein expression and collagen organization in the matrix under basal conditions and that epithelial injury can increase the concentration of TGF-β2 approximately twofold and induce changes in the matrix that are consistent with subepithelial fibrosis. These results suggest a prominent role for the epithelium in modulating basal and wound-healing matrix homeostasis and that tight regulation of epithelial-derived TGF-β2 may be necessary for normal EMTU function.

## REFERENCES

1. **Agarwal A, Coleno ML, Wallace VP, Wu WY, Sun CH, Tromberg BJ, and George SC.** Two-photon laser scanning microscopy of epithelial cell-modulated collagen density in engineered human lung tissue. *Tissue Eng* 7: 191–202, 2001.

2. **Agarwal AR, Mih J, and George SC.** Expression of matrix proteins in an in vitro model of airway remodeling in asthma. *Allergy Asthma Proc* 24: 35–42, 2003.

3. **Balzar S, Chu HW, Silkoff P, Cundall M, Trudeau JB, Strand M, and Wenzel S.** Increased TGF-β2 in severe asthma with eosinophilia. *J Allergy Clin Immunol* 115: 110–117, 2005.

4. **Bell E, Ehrlich HP, Buttle DJ, and Nakatsuji T.** Living tissue formed in vitro and accepted as skin-equivalent tissue of full thickness. *Science* 211: 1052–1054, 1981.

5. **Bhowmick NA, Chytil A, Plieth D, Gorska AE, Dumont N, Shappell S, Washington MK, Neilson EG, and Moses HL.** TGF-β signaling in fibroblasts modulates the oncogenic potential of adjacent epithelia. *Science* 303: 848–851, 2004.

6. **Biecker E, De Gottardi A, Neef M, Unternahrer M, Schneider V, Ledermann M, Sagesser H, Shaw S, and Reichen J.** Long-term treatment of bile duct-ligated rats with rapamycin (sirolimus) significantly attenuates liver fibrosis: analysis of the underlying mechanisms. *J Pharmacol Exp Ther* 313: 952–961, 2005.

7. **Birukova AA, Birukov KG, Adyshev D, Usatyuk P, Natarajan V, Garcia JG, and Verin AD.** Involvement of microtubules and Rho pathway in TGF-β1-induced lung vascular barrier dysfunction. *J Cell Physiol* 204: 934–947, 2005.

8. **Bradford MM.** A rapid and sensitive method for the quantitation of microgram quantities of protein utilizing the principle of protein-dye binding. *Anal Biochem* 72: 248–254, 1976.

9. **Cambrey AD, Kwon OJ, Gray AJ, Harrison NK, Yacoub M, Barnes PJ, Laurent GJ, and Chung KF.** Insulin-like growth factor I is a major fibroblast mitogen produced by primary cultures of human airway epithelial cells. *Clin Sci (Lond)* 89: 611–617, 1995.

10. **Campbell JH and Campbell GR.** Endothelial cell influences on vascular smooth muscle phenotype. *Annu Rev Physiol* 48: 295–306, 1986.

11. **Cheng N, Bhowmick NA, Chytil A, Gorksa AE, Brown KA, Muraoka R, Arteaga CL, Neilson EG, Hayward SW, and Moses HL.** Loss of TGF-β type II receptor in fibroblasts promotes mammary carcinoma growth and invasion through upregulation of TGF-α-, MSP- and HGF-mediated signaling networks. *Oncogene* 24: 5053–5068, 2005.

12. **Chiquet-Ehrismann R.** Tenascin and other adhesion-modulating proteins in cancer. *Semin Cancer Biol* 4: 301–310, 1993.

13. **Choe MM, Sporn PH, and Swartz MA.** An in vitro airway wall model of remodeling. *Am J Physiol Lung Cell Mol Physiol* 285: L427–L433, 2003.

14. **Davies DE, Wicks J, Powell RM, Puddicombe SM, and Holgate ST.** Airway remodeling in asthma: new insights. *J Allergy Clin Immunol* 111: 215–225; quiz 226, 2003.

15. **Demayo F, Minoo P, Plopper CG, Schuger L, Shannon J, and Torday JS.** Mesenchymal-epithelial interactions in lung development and repair: are modeling and remodeling the same process? *Am J Physiol Lung Cell Mol Physiol* 283: L510–L517, 2002.

16. **Desmouliere A, Darby IA, and Gabbiani G.** Normal and pathologic soft tissue remodeling: role of the myofibroblast, with special emphasis on liver and kidney fibrosis. *Lab Invest* 83: 1689–1707, 2003.

17. **Dombkowski KJ, Wasilevich EA, and Lyon-Callo SK.** Pediatric asthma surveillance using Medicaid claims. *Public Health Rep* 120: 515–524, 2005.

18. **Dunn AK, Wallace VP, Coleno M, Berns MW, and Tromberg BJ.** Influence of optical properties on two-photon fluorescence imaging in turbid samples. *Appl Opt* 39: 1–8, 2000.

19. **Durr RA, Dubaybo BA, and Thet LA.** Repair of chronic hyperoxic lung injury: changes in lung ultrastructure and matrix. *Exp Mol Pathol* 47: 219–240, 1987.

20. **Erickson HP and Bourdon MA.** Tenascin: an extracellular matrix protein prominent in specialized embryonic tissues and tumors. *Annu Rev Cell Biol* 5: 71–92, 1989.

21. **Evans MJ, Van Winkle LS, Fanucchi MV, and Plopper CG.** The attenuated fibroblast sheath of the respiratory tract epithelial-mesenchymal trophic unit. *Am J Respir Cell Mol Biol* 21: 655–657, 1999.

22. **Evans MJ, Van Winkle LS, Fanucchi MV, and Plopper CG.** Cellular and molecular characteristics of basal cells in airway epithelium. *Exp Lung Res* 27: 401–415, 2001.

23. **Evans RA, Tian YC, Steadman R, and Phillips AO.** TGF-β1-mediated fibroblast-myofibroblast terminal differentiation-the role of Smad proteins. *Exp Cell Res* 282: 90–100, 2003.

24. **Evans SE, Colby TV, Ryu JH, and Limper AH.** Transforming growth factor-β 1 and extracellular matrix-associated fibronectin expression in pulmonary lymphangioleiomyomatosis. *Chest* 125: 1063–1070, 2004.

25. **Galiacy S, Planus E, Lepetit H, Fereol S, Laurent V, Ware L, Isabey D, Matthay M, Harf A, and d'Ortho MP.** Keratinocyte growth factor promotes cell motility during alveolar epithelial repair in vitro. *Exp Cell Res* 283: 215–229, 2003.

26. **Georgiou E, Theodossiou T, Hovhannisyan V, Politopoulos K, Rapti GS, and Yova D.** Second and third optical harmonic generation in type I collagen by nanosecond laser irradiation, over a broad spectral region. *Opt Commun* 176: 253–260, 2000.

27. **Holgate ST.** Epithelial damage and response. *Clin Exp Allergy* 30 Suppl 1: 37–41, 2000.

28. **Holgate ST, Davies DE, Lackie PM, Wilson SJ, Puddicombe SM, and Lordan JL.** Epithelial-mesenchymal interactions in the pathogenesis of asthma. *J Allergy Clin Immunol* 105: 193–204, 2000.

29. **Holgate ST, Peters-Golden M, Panettieri RA, and Henderson WR Jr.** Roles of cysteinyl leukotrienes in airway inflammation, smooth muscle function, and remodeling. *J Allergy Clin Immunol* 111: S18–S34; discussion S34–S36, 2003.

30. **Kaarteenaho-Wiik R, Kinnula VL, Herva R, Soini Y, Pollanen R, and Paakko P.** Tenascin-C is highly expressed in respiratory distress syndrome and bronchopulmonary dysplasia. *J Histochem Cytochem* 50: 423–431, 2002.

31. **Kaarteenaho-Wiik R, Lakari E, Soini Y, Pollanen R, Kinnula VL, and Paakko P.** Tenascin expression and distribution in pleural inflammatory and fibrotic diseases. *J Histochem Cytochem* 48: 1257–1268, 2000.

32. **Li YH, Chen M, Brauner A, Zheng C, Skov Jensen J, and Tullus K.** Ureaplasma urealyticum induces apoptosis in human lung epithelial cells and macrophages. *Biol Neonate* 82: 166–173, 2002.

33. **Mackie EJ, Halfter W, and Liverani D.** Induction of tenascin in healing wounds. *J Cell Biol* 107: 2757–2767, 1988.

34. **Menke A and Adler G.** TGFβ-induced fibrogenesis of the pancreas. *Int J Gastrointest Cancer* 31: 41–46, 2002.

35. **Mio T, Liu XD, Adachi Y, Striz I, Skold CM, Romberger DJ, Spurzem JR, Illig MG, Ertl R, and Rennard SI.** Human bronchial epithelial cells modulate collagen gel contraction by fibroblasts. *Am J Physiol Lung Cell Mol Physiol* 274: L119–L126, 1998.

36. **Nakamura Y, Tate L, Ertl RF, Kawamoto M, Mio T, Adachi Y, Romberger DJ, Koizumi S, Gossman G, Robbins RA, Spurzem JR, and Rennard SI.** Bronchial epithelial cells regulate fibroblast proliferation. *Am J Physiol Lung Cell Mol Physiol* 269: L377–L387, 1995.

37. **Nawshad A, LaGamba D, and Hay ED.** Transforming growth factor β (TGFβ) signaling in palatal growth, apoptosis and epithelial mesenchymal transformation (EMT). *Arch Oral Biol* 49: 675–689, 2004.

38. **Paakko P, Kaarteenaho-Wiik R, Pollanen R, and Soini Y.** Tenascin mRNA expression at the foci of recent injury in usual interstitial pneumonia. *Am J Respir Crit Care Med* 161: 967–972, 2000.

39. **Parry TJ, Brosius R, Thyagarajan R, Carter D, Argentieri D, Falotico R, and Siekierka J.** Drug-eluting stents: sirolimus and paclitaxel differentially affect cultured cells and injured arteries. *Eur J Pharmacol*, 2005.

40. **Pilot F and Lecuit T.** Compartmentalized morphogenesis in epithelia: from cell to tissue shape. *Dev Dyn* 232: 685–694, 2005.

41. **Puddicombe SM, Polosa R, Richter A, Krishna MT, Howarth PH, Holgate ST, and Davies DE.** Involvement of the epidermal growth factor receptor in epithelial repair in asthma. *FASEB J* 14: 1362–1374, 2000.

42. **Rees J.** ABC of asthma. Prevalence. *BMJ* 331: 443–445, 2005.

43. **Rennard SI, Romberger DJ, Sisson JH, Von Essen SG, Rubinstein I, Robbins RA, and Spurzem JR.** Airway epithelial cells: functional roles in airway disease. *Am J Respir Crit Care Med* 150: S27–S30, 1994.

44. **Richter A, Puddicombe SM, Lordan JL, Bucchieri F, Wilson SJ, Djukanovic R, Dent G, Holgate ST, and Davies DE.** The contribution of interleukin (IL)-4 and IL-13 to the epithelial-mesenchymal trophic unit in asthma. *Am J Respir Cell Mol Biol* 25: 385–391, 2001.

45. **Roche WR, Beasley R, Williams JH, and Holgate ST.** Subepithelial fibrosis in the bronchi of asthmatics. *Lancet* 1: 520–524, 1989.

46. **Sanford LP, Ormsby I, Gittenberger-de Groot AC, Sariola H, Friedman R, Boivin GP, Cardell EL, and Doetschman T.** TGFβ2 knockout

mice have multiple developmental defects that are non-overlapping with other TGFβ knockout phenotypes. *Development* 124: 2659–2670, 1997.

47. **Shoji S, Rickard KA, Ertl RF, Robbins RA, Linder J, and Rennard SI.** Bronchial epithelial cells produce lung fibroblast chemotactic factor: fibronectin. *Am J Respir Cell Mol Biol* 1: 13–20, 1989.

48. **Swartz MA, Tschumperlin DJ, Kamm RD, and Drazen JM.** Mechanical stress is communicated between different cell types to elicit matrix remodeling. *Proc Natl Acad Sci USA* 98: 6180–6185, 2001.

49. **Tamaoki M, Imanaka-Yoshida K, Yokoyama K, Nishioka T, Inada H, Hiroe M, Sakakura T, and Yoshida T.** Tenascin-C regulates recruitment of myofibroblasts during tissue repair after myocardial injury. *Am J Pathol* 167: 71–80, 2005.

50. **Ten Hacken NH, Postma DS, and Timens W.** Airway remodeling and long-term decline in lung function in asthma. *Curr Opin Pulm Med* 9: 9–14, 2003.

51. **Tschumperlin DJ, Shively JD, Kikuchi T, and Drazen JM.** Mechanical stress triggers selective release of fibrotic mediators from bronchial epithelium. *Am J Respir Cell Mol Biol* 28: 142–149, 2003.

52. **Watanabe S, Hirose M, Wang XE, Kobayashi O, Nagahara A, Murai T, Iwazaki R, Miwa H, Miyazaki A, and Sato N.** Epithelial-mesenchymal interaction in gastric mucosal restoration. *J Gastroenterol* 35 *Suppl* 12: 65–68, 2000.

53. **Wen FQ, Kohyama T, Liu X, Zhu YK, Wang H, Kim HJ, Kobayashi T, Abe S, Spurzem JR, and Rennard SI.** Interleukin-4- and interleukin-13-enhanced transforming growth factor-β2 production in cultured human bronchial epithelial cells is attenuated by interferon-γ. *Am J Respir Cell Mol Biol* 26: 484–490, 2002.

54. **Wen FQ, Liu X, Kobayashi T, Abe S, Fang Q, Kohyama T, Ertl R, Terasaki Y, Manouilova L, and Rennard SI.** Interferon-γ inhibits transforming growth factor-β production in human airway epithelial cells by targeting Smads. *Am J Respir Cell Mol Biol* 30: 816–822, 2004.

55. **Williams RM, Zipfel WR, and Webb WW.** Interpreting second-harmonic generation images of collagen I fibrils. *Biophys J* 88: 1377–1386, 2005.

56. **Wilson SE, Liu JJ, and Mohan RR.** Stromal-epithelial interactions in the cornea. *Prog Retin Eye Res* 18: 293–309, 1999.

57. **Wong BJ, Wallace V, Coleno M, Benton HP, and Tromberg BJ.** Two-photon excitation laser scanning microscopy of human, porcine, and rabbit nasal septal cartilage. *Tissue Eng* 7: 599–606, 2001.

58. **Zagzag D, Friedlander DR, Miller DC, Dosik J, Cangiarella J, Kostianovsky M, Cohen H, Grumet M, and Greco MA.** Tenascin expression in astrocytomas correlates with angiogenesis. *Cancer Res* 55: 907–914, 1995.

59. **Zhu J, Wu J, Frizell E, Liu SL, Bashey R, Rubin R, Norton P, and Zern MA.** Rapamycin inhibits hepatic stellate cell proliferation in vitro and limits fibrogenesis in an in vivo model of liver fibrosis. *Gastroenterology* 117: 1198–1204, 1999.

60. **Zhu S, Goldschmidt-Clermont PJ, and Dong C.** Transforming growth factor-β-induced inhibition of myogenesis is mediated through Smad pathway and is modulated by microtubule dynamic stability. *Circ Res* 94: 617–625, 2004.

61. **Zoumi A, Yeh A, and Tromberg BJ.** Imaging cells and extracellular matrix in vivo by using second-harmonic generation and two-photon excited fluorescence. *Proc Natl Acad Sci USA* 99: 11014–11019, 2002.